AAEC/E205

AAEC/E205

AUSTRALIAN ATOMIC ENERGY COMMISSION
RESEARCH ESTABLISHMENT
LUCAS HEIGHTS

COLLISION PROBABILITY CALCULATIONS IN CLUSTER GEOMETRY

by

G. DOHERTY

March 1970

AUSTRALIAN ATOMIC ENERGY COMMISSION

RESEARCH ESTABLISHMENT

LUCAS HEIGHTS

COLLISION PROBABILITY CALCULATIONS IN CLUSTER GEOMETRY

by

G. DOHERTY

ABSTRACT

Four methods for the calculation of multigroup collision probabilities in cluster geometry are described. These are Monte Carlo, full numerical integration, numerical integration over the annuli containing rods combined with the Bonalumi approximation in the moderator annuli, and a ring smearing method again based on the Bonalumi approximation for annular geometry. Results of six group calculations for three tight, natural uranium, D_2O lattices are presented in detail.

These results suggest that the ring smearing model is suitable for cluster calculations which do not require high accuracy. The largest error is in the thermal flux in the outer moderator regions. This error is a general problem inherent in the Bonalumi approximation and is not peculiar to the ring smearing model presented.

CONTENTS

1. INTRODUCTION

Collision probability methods offer some significant advantages in cluster geometry neutron flux calculations. The alternative diffusion and Sn transport methods suffer from the fact that the individual fuel pins cannot be represented explicitly, and some sort of smearing model has to be devised. As a general principle in transport calculations we want to be able to obtain as accurate an answer as is required, simply by increasing the number of groups in the multigroup representation, or the number of mesh intervals and angles in the spatial flux representation. Such a refinement procedure cannot be adopted when smearing models are employed, because the error inherent in the smearing approximation always remains. The collision probability method with its explicit representation of fuel pins does meet this refinement criterion satisfactorily, and is therefore popular in calculations with cluster cells.

The collision probability method consists essentially of two independent steps – the calculation of the multigroup collision probability matrices, and the solution of the neutron balance equations for the multigroup region fluxes. Of these the calculation of the collision probability matrices takes a major part of the total calculation time, while the flux solution process is carried out using standard iterative techniques (Pull 1963, Doherty 1969 a) which are common to all collision probability calculations.

The present report discusses various methods for calculating the collision probability matrices which have been programmed for the IBM360/50H computer, and presents a comparison of accuracies and computing times obtained for some typical cells using the different methods.

2. MONTE CARLO METHODS

The collision probability P_{ij} is defined to be the probability that a neutron born uniformly in volume and isotropically in angle within region i will have its next collision in region j. Figure 1 shows a typical cluster lattice cell and we assume for simplicity that the regions to be used in the collision probability calculation are the physically distinct regions shown in the figure. As we have previously remarked, the physical regions of the cell may be subdivided to improve the spatial flux representation in an actual calculation. However, the physical regions in the figure already include all the geometric complexities we wish to discuss.

We note first that the outer boundary of the moderator in Figure 1 is square. For this problem, and for a hexagonal outer boundary, it is convenient to replace this boundary by a circular one containing the same volume of moderator. This approximation, when used with the assumption that neutrons leaving the cell are reflected isotropically (white boundary condition) has been shown to give adequate accuracy in cells not containing clusters (Doherty 1969 b) and the same accuracy will be obtained here. With such a circular outer boundary the six fuel pins in the outer ring are physically equivalent, and for the purpose of computing the fluxes they may be regarded as one region with six times the volume. In the calculation of the collision probability matrices, they will, of course, be treated individually.

2.1 Direct Simulation Monte Carlo

The most direct and simple method of calculating collision probabilities is the direct simulation Monte Carlo method. This process consists of sampling for a set of initial starting coordinates and direction cosines, then sampling for a neutron tracking distance in mean free paths, stepping off the track length through the regions of various total cross section until the collision point is established, and finally scoring the collision in the appropriate box. Then if N_i neutrons are started out of region i, and of these, N_{ij} have their collision points in region j, the collision probability P_{ij} is estimated to be

$$P_{ij} = N_{ij}/N_i \quad .$$

Provided the number N_{ij} is high enough for successive trials with N_i neutrons to yield a normal distribution of values of N_{ij}, the standard deviation in N_{ij} is simply

$$N_{ij} = \sqrt{N_i P_{ij} (1-P_{ij})} \quad .$$

Thus the estimate P_{ij} can be assigned an error on the basis of one trial of N_i neutrons:

$$P_{ij} = \sqrt{N_{ij}/N_i \pm P_{ij}\,(1-P_{ij})/N_i} \quad .$$

As is customary in Monte Carlo calculations, the error goes down only as the square root of the sample size so that obtaining sufficient accuracy usually requires a very rapid tracking procedure, or a large amount of computing time.

2.2 Sampling Techniques

The sampling procedure is to select a set of neutron starting coordinates, a set of direction cosines, and finally a neutron track length in mean free paths. In the cluster geometry we are considering, no account is taken of axial dependence in the collision probability calculation, so it is unnecessary to select z coordinate starting values. The selection of starting x, y coordinates is governed by the requirement that sufficient neutrons be started out of each region to ensure that the P_{ij} errors will be acceptable. The Monte Carlo process actually calculates the larger collision probabilities with better accuracy than the smaller ones, which is generally a desirable feature though it poses problems if accurate reaction rates are required in a small region.

To ensure that sufficient neutrons are started out of each region in the problem, the routine as programmed requires specification of the number of neutrons which are to be started out of each annulus. For the physical regions of Figure 1, the coolant region contains all the fuel pins and therefore requires a larger number of neutrons to be started there to obtain adequate statistics on the coolant and fuel pin collision probabilities. Neutrons must be started uniformly in volume, which can be accomplished either by rejection or by direct sampling.

Let the inner and outer radii of an annulus be r_1 and r_2 respectively and let a_i be a set of random numbers on the interval (0,1). The rejection algorithm may be simply stated:

$$x = r_2\,(1 - 2a_1)$$

$$y = r_2\,(1 - 2a_2)$$

$$x^2 + y^2 > r_2^2 \quad \text{reject}$$

$$x^2 + y^2 < r_1^2 \quad \text{reject} \quad .$$

This algorithm has the advantage that x,y are defined explicitly in the selection process. Restriction to any one of the four angular quadrants is simply accomplished by altering the equation for x,y. For example, if we require $x > 0$, $y > 0$, then

$$x = r_2\, a_1$$

$$y = r_2\, a_2$$

will achieve this result. However, it may be desirable to restrict x,y to lie within some other angular segment to improve the variance of our results by explicitly including geometry symmetries present in the problem. In the seven rod cluster of Figure 1, the starting position of neutrons can be restricted to the angular interval $(0, \frac{\pi}{6})$ from symmetry. Such a restriction is difficult to implement using a rejection technique.

The efficiency ϵ of the rejection technique is defined as the number of acceptable starting coordinates divided by the total number of trials. From area considerations this quantity can be seen to be:

$$\epsilon = \frac{\pi}{4}\,\frac{r_2^2 - r_1^2}{r_2^2} \quad ,$$

if the whole area of the annulus is to be sampled. In the outer annuli the efficiency ϵ is too small to make the rejection approach attractive.

The direct sampling procedure is to select a radius r from the probability distribution

$$P(r)\,dr = \frac{2r\,dr}{r_2^2 - r_1^2} \quad ,$$

and an angle θ from the angular segment $(0, \phi)$ determined by symmetry considerations:

$$r = [r_1^2 + (r_2^2 - r_1^2)\,a_1\,]^{1/2}$$

$$\theta = \phi\, a_2$$

$$x = r \cos\theta$$

$$y = r \sin\theta \ .$$

Rejection techniques are available for the simple square root and for sin and cos when θ is unrestricted, but these are inconvenient to apply on annuli with restricted angular segments.

Next a set of direction cosines for the neutron track must be selected. Rejection techniques are standard for this task when either (α, β) or (α, β, γ) are required. In this programme the axial dependence will be treated by integration so we need only select (α, β). The neutron will be tracked in both forward and backward directions, so we need only consider set $\beta > 0$. The rejection algorithm is then

$$c = a_1$$

$$d = a_2 \ ,$$

if $c^2 + d^2 > 1$ reject

$$\alpha = \frac{c^2 - d^2}{c^2 + d^2}$$

$$\beta = \frac{2\,c\,d}{c^2 + d^2} \ .$$

The efficiency is $\frac{\pi}{4}$ which is usually sufficient to ensure that rejection will be computationally faster than direct sampling.

2.3 Tracking Techniques

In direct simulation Monte Carlo, a neutron track length d in mean free paths is selected from the distribution

$$P(d) = e^{-d} \ ,$$

and this mean free path distance is stepped off along the direction cosines selected, using the total cross sections of the regions through which the track passes until a collision point is reached. In the present application, it is intended that more than one energy group will be considered so we are faced with two unattractive alternatives; either each energy group must be considered separately with the implied duplication of selection processes and tracking, or the stepping off problem is complicated by the need to consider simultaneously the total cross sections for all groups. The cluster is often quite tight and the identification of points of intersection between the neutron track and region boundaries is a non-trivial problem, so a multiple stepping off process is clearly inefficient.

A device which has achieved some success in one group cluster collision probability calculations is the virtual collision probability method of Woodcock et al. (1965) used in the MONTE programme described by McCulloch et al. (1968). Essentially the intersection point problem is avoided by taking all total cross sections equal to the largest so that the tracking problem resolves itself into identifying the finishing point which is a much simpler task. The collision point can be real if the total cross section equals the largest total cross section in the system, otherwise the weight of the neutron is reduced, a partial collision is scored, and tracking continues. The method is successful if all the cross sections in the system are roughly of the same order of magnitude, a situation which unfortunately does not prevail in multigroup calculations. Even if this were not so, the prospect of tracking terminating in some groups and continuing in others is uninviting, as this would considerably impair the efficiency of the overall calculation.

The best solution is to admit the tracking complexity and set up an efficient procedure for determining all the intercepts from one side of the cluster to the other. Having done this once, we can abandon direct simulation tracking and instead of scoring only a collision in one region we can, without much additional labour, score for each region an estimated collision probability. This estimator device is discussed by Pull (1962) and is known to give worthwhile reductions in variance. With the estimator approach we have additional information necessary to integrate in the axial direction, thus eliminating this potentially large source of statistical error. The precise form of the estimator is discussed below.

2.4 The Intercept Calculation

All the region surfaces in the cluster problem are circular so all intercept calculations are of the same type. The equations of the track are simply

$$x = x_0 + \alpha t$$

$$y = y_0 + \beta t \quad .$$

We assume for simplicity that a typical circle of radius r is centred at the origin, as translation to any other centre is trivially achieved.

$$x^2 + y^2 = r^2 \quad .$$

If

$$p^2 = (\alpha x_0 + \beta y_0)^2 + r^2 - (x_0^2 + y_0^2) ,$$

then the track intersects the circle if $p^2 > 0$ with signed values of t given by

$$t = -(\alpha x_0 + \beta y_0) \pm p \quad .$$

Each of the circular surfaces in the cluster can be examined in turn, using simple geometric properties to exclude unnecessary testing. In this way we can build up an array of intersections t_i with a corresponding set of region identifiers m_i . It is unwise to attempt to sort these into order while the circles are being examined because the sorting can be done efficiently using a machine language coded, bit pattern sort when the full array of intersection points has been assembled. Such a sort routine is usually available at any large computing installation and is, in any case, not difficult to write.

With the intersection points ordered into ascending order, it is a simple matter to deduce the track lengths in each region across the cluster. If the coolant regions are subdivided and do not enclose all the rods, the logic is slightly more complicated as some intersection points with coolant boundaries may be internal to rods. Having established the track lengths the problem is reduced to computing the probability estimators.

2.5 The Probability Estimator

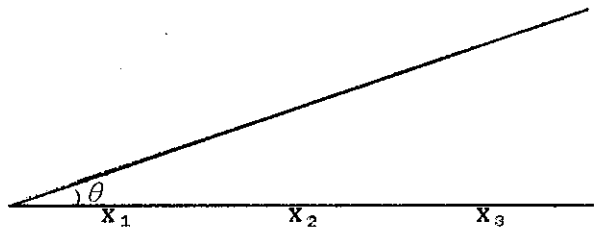

Suppose the neutron track has successive intercepts x_1, x_2, x_3--- with regions of cross section $\Sigma_1, \Sigma_2, \Sigma_3$---. The transmission probability at an angle θ to the horizontal plane through a distance x in material with cross section Σ is

$$e^{\frac{-x\Sigma}{\cos\theta}} .$$

The probability that a neutron will be born in an interval $d\theta$ about an angle θ to the horizontal plane is

$$P(\theta)\, d\theta = \cos\theta\, d\theta .$$

Thus the collision probabilities from the starting point q to each of the regions is given by

$$P_{q1} = \int_0^{\frac{\pi}{2}} \left[1 - e^{-x_1 \Sigma_1/\cos\theta}\right] \cos\theta\, d\theta ,$$

$$P_{q2} = \int_0^{\frac{\pi}{2}} e^{-x_1 \Sigma_1/\cos\theta} \left[1 - e^{-x_2 \Sigma_2/\cos\theta}\right] \cos\theta\, d\theta ,$$

Each of the estimators requires the evaluation of the K_{i2} function

$$K_{i2}(y) = \int_0^{\frac{\pi}{2}} e^{-y/\cos\theta} \cos\theta\, d\theta ,$$

for which fast and accurate subroutines are given by a number of authors, for example, Gargantini and Pomentale (1964). Thus:

$$P_{q1} = 1 - K_{i2}(x_1 \Sigma_1) ,$$

$$P_{q2} = K_{i2}(x_1 \Sigma_1) - K_{i2}(x_1 \Sigma_1 + x_2 \Sigma_2) ,$$

All groups in the problem can now be treated with equal ease, requiring only a change of cross section in the estimator. Thus instead of the original concept of a set of finishers N_{ij} resulting from N_i starters in region i, the N_{ij} now contain the estimated number of finishers. Division by N_i produces the final collision probability matrix, completing the calculation.

2.6 Discussion

The final form of the Monte Carlo routine is now far removed from the simple idea of direct neutron tracking. Random numbers intrude into the calculation only in the selection of the neutron starting point and its direction cosines in the plane. Efficiency considerations have dictated the development of the rather elaborate tracking scheme which has been devised, but it is clear that the tracking procedure yields much more information than can be utilised by the simple starter-finisher philosophy. The same intercepts should be used to provide collision probability contributions for every point which the Monte Carlo process has selected as the starting point of the neutrons. It is also clear that by selecting the orientation of the tracks and assigning variable weights corresponding to a simple integration scheme, the problem of reducing the variance in the Monte Carlo calculation can be transformed into the more familiar problem of obtaining a desired accuracy from an integration algorithm. The numerical integration scheme discussed in the next section is thus preferable as a routine calculation, though the Monte Carlo method provides a useful check on the correctness of the numerical integration routine.

3. NUMERICAL INTEGRATION METHOD

The numerical integration method consists of laying down a set of parallel neutron tracks at a number of discrete angular orientations to a reference diameter of the cluster, and integrating along each track to produce collision probabilities for the different regions. We have two numerical integrations to perform; the radial integration across the cluster, and the integration over track orientations. The radial integration is defined by the number of tracks per annulus. If n_1 tracks are to be placed across the annulus (r_1, r_2) then with

$$\Delta = (r_2 - r_1)/n_1 ,$$

tracks are placed at distances from the centre given by

$$r = r_1 + \Delta/2$$

$$r = r_1 + 3\Delta/2$$

$$\text{- - - - - - -}$$

$$r = r_1 + \overline{2n-1}\,\Delta/2 ,$$

and each track is given equal weight Δ on the integration.

Specifying the number of tracks per annulus ensures that no region escapes refinement when the total number of tracks in the problem is increased, offering a conceptual advantage over the alternative method of equal spacing across the entire cluster. The latter does not guarantee a refinement of small regions when the number of tracks is increased. For tracks which do not intersect annuli containing rods, the intercepts are independent of the angular orientation of the track, so the angular integration is not required for the outer annuli. If the number of tracks per annulus is specified, the angular integration can be deleted conveniently. The track intercepts can be used to compute the volumes of the various regions using the same quadrature scheme as is used to compute the collision probabilities, and a comparison of the actual and computed volumes yields quite a good assessment of the accuracy with which the collision probabilities are being computed.

The angular integration is performed over the range $(0, \phi/2)$ where ϕ is the rotational symmetry angle of the cluster. In the seven rod cluster of Figure 1, $\phi = \frac{\pi}{3}$. Provided that the number of angles is relatively prime to the number of rods on each pitch circle, the range of integration $(0, 2\pi)$ gives an equivalent representation to $(0, \phi/2)$ and avoids the possibility of input error. The range of integration is broken into equal angular segments with the track angle at the centre of the segment. The tracks are again equally weighted, corresponding to the physical situation where all neutron directions are equally likely. The reason for using equal weighting in the radial integration is quite different. Here a more complicated integration rule, such as Gauss-Legendre quadrature, could profitably be used if the rod

intercepts t(r) were non-zero over the width of an annulus $r_1 < r < r_2$. Unfortunately such is not the case and one is forced to use equally spaced, equally weighted tracks to ensure that the errors are uniformly reduced when the number of tracks is increased.

The tracking procedure is precisely that outlined in Section 2.4 for the Monte Carlo calculation. Each track yields a set of intercepts t_i with regions m_i and again the collision probabilities can be expressed in terms of a Bessel function integral. In the Monte Carlo calculation we calculated the point-to-region probabilities from the specific starting point on the track which was selected. In this calculation we perform analytically the integration over starting position in each intercept to compute region-to-region probabilities.

3.1 The Numerical Integration Formulae

The collision probability from region i to region j may be written

$$P_{ij} = \frac{1}{V_i} \int_{V_i} d\underset{\sim}{t}_i \int_{V_j} d\underset{\sim}{t}_j \; P(\underset{\sim}{t}_i, \underset{\sim}{t}_j) \; ,$$

where $\underset{\sim}{t}_i$ defines a point in region i

and V_i is the volume of region i .

The point to point collision probability $P(t_i, t_j)$ is given by the relation

$$P(\underset{\sim}{t}_i, \underset{\sim}{t}_j) = \Sigma_j \, e^{-P} \; ,$$

where p is the path length (in mean free paths) from $\underset{\sim}{t}_i$ to $\underset{\sim}{t}_j$.

The system under consideration is infinite in the axial direction so that z integration in dt_i can be ignored. Using the method of parallel tracks described above, the double integral in P_{ij} may be written:

$$P_{ij} = \frac{\int_0^R dx \int_0^{\phi} d\phi \int_0^{\frac{\pi}{2}} \sin\theta \, d\theta \int_0^{t_i} dy_i \int_0^{t} dy_j \quad P(y_i, y_j)}{\int_0^R dx \int_0^{\phi} d\phi \int_0^{\frac{\pi}{2}} \sin\theta \, d\theta \; t_i} \; ,$$

where R is the outer boundary of the system,

ϕ is the angle in the radial plane between the neutron track and the reference diameter,

θ is the angle between the neutron track and the vertical axis,

t_i is the intercept of the neutron track with region i,

t_j is the intercept of the neutron track with region j,

$P(y_i, y_j)$ is the probability that a neutron starting at y_i on intercept t_i will collide at y_j on intercept t_j .

If there are a number of intervening regions k this probability is simply:

$$P(y_i, y_j) = e^{-\Sigma_i (t_i - y_i)/\sin\theta} \prod_K e^{-\Sigma_k t_k/\sin\theta} \frac{\Sigma_j}{\sin\theta} e^{-\Sigma_j y_j/\sin\theta}$$

$$\int_0^{t_j} P(y_i, y_j)\, dy_i = e^{-\Sigma_i (t_i - y_i)/\sin\theta} \prod_K e^{-\Sigma_k t_k/\sin\theta} \left[1 - e^{-\Sigma_j t_j/\sin\theta}\right]$$

$$\int_0^{t_i} dy_i \int_0^{t_j} dy_j\, P(y_i, y_j) = \frac{\sin\theta}{\Sigma_i} \left[1 - e^{-\Sigma_i t_i/\sin\theta}\right] \prod_K e^{-\Sigma_k t_k/\sin\theta} \left[1 - e^{-\Sigma_j t_j/\sin\theta}\right].$$

The integrations which must be performed are of the type

$$\int_0^{\frac{\pi}{2}} \sin^2\theta\ e^{-x/\sin\theta}\, d\theta = K_{i3}(x) \quad ,$$

for which accurate subroutines have been given by Clayton (1964) and Gargantini and Pomentale (1964).

3.2 Selection of the Number of Tracks and the Number of Angles

The numerical integration procedure which we have described is quite time consuming since each track gives us a set of intercepts t and for every pair t_i, t_j of these a contribution requiring the evaluation of four K_{i3} terms must be made to the appropriate P_{ij} for every energy group of the multigroup representation. Consequently there is a considerable interest in obtaining the minimum number of tracks per annulus and angles which will yield collision probabilities of the desired accuracy.

The volumes of the regions are computed together with the collision probabilities, being the denominator of the P_{ij}. If we ignore for a moment those annuli which do not intersect or enclose fuel pins, the volumes of the remaining annuli show a steady increase in accuracy with increasing number of tracks per annulus. It is thus simple to arrive at a number of tracks per annulus which will satisfactorily describe these simple annuli, using only one angle in the integration. The calculation of the fuel rod volumes, and the volumes of the annuli immediately adjacent to them, will not be sufficiently accurate when only one angle is employed, and we can increase the number of angles, keeping the number of tracks per annulus constant, until the volumes of these regions reach satisfactory accuracy. In this way a systematic search for the minimum track-angle representation can be undertaken for each type of cluster. When the necessary computational effort has been invested on a number of different cluster configurations, experience will suffice to provide the user with appropriate values of these two numbers. Such experimentation is necessary because the time is proportional to the product of the two numbers and we cannot afford to be too generous with either of them.

Some numerical results which will provide useful guidelines for efficient use of the subroutine are provided in a later section. It will be seen that the times for use of the subroutine are unsatisfactory for day-to-day calculations and there is considerable incentive to provide a faster routine which retains as much of the accuracy of the numerical integration procedure as possible. A similar numerical integration routine PIJ which was described by Beardwood et al. (1965) is now incorporated in the multigroup lattice code WIMS (Askew et al. 1966) on which running experience has been accumulated over a number of years. The current version of PIJ contains a facility for computing collision probabilities in the outer annuli of the cluster using the methods developed by Bonalumi (1961) which yield worthwhile savings of computer time. The theory of such an approximation is presented in the next section.

4. USE OF THE BONALUMI METHOD IN THE OUTER ANNULI

The use of the approximation is confined to probabilities for those annuli which are completely external to the fuel pins. The fuel pins are smeared into surrounding annuli and a normal Bonalumi calculation is performed on the annular system which smearing has formed. Details of the equations which are solved are presented in Section 4.2, where the modifications required to cope with void annuli are also discussed. If i and j index annular regions, the Bonalumi treatment gives us a set of collision probabilities P'_{ij} and a set of ring capture probabilities G'_{ij} . The quantities G'_{ij} arise naturally in the Bonalumi theory and are defined as follows:

G'_{ij} = the probability that a neutron born in region i , and arriving at the inner boundary of annulus j will collide in region j .

The quantities G'_{ij} vary slowly with the position of the annulus i so that if i is a smeared annulus then G'_{ij} will apply equally well to both the coolant and the rods which make up the smeared annulus .

An annular boundary r_i is chosen so that all the rods are contained inside r_i . The collision probabilities for the regions enclosed by r_i are then computed by the numerical integration method discussed in Section 3. At the end of this step, the following quantities will be available:

$$P_{jk} \quad \text{for} \quad j,k \leqslant i$$

$$P_{jr_i} = 1 - \underset{k \leqslant i}{\text{Sum}} P_{jk}$$

(The j,k indices are assumed to include in their range all the fuel rods and their subdivisions, as well as the annuli internal to i).

Thus we have from the Bonalumi calculation, P_{jk} for $j,k > i$ and from the numerical integration P_{jk} for $j,k \leqslant i$. It remains only to show the form of P_{jk} for $j \leqslant i$, $k > i$ as P_{kj} will be obtained by reciprocity.

P_{jr_i} is the probability that a neutron will arrive at the internal boundary of annulus P_{i+1}. Hence

$$P_{j\,i+1} = P_{j\,r_i}\, G'_{j\,i+1}$$

– – – – – – – – – – –

$$P_{jk} = P_{j\,r_i} (1 - G'_{j\,i+2}) \cdots (1 - G'_{j\,k-1})\, G_{jk} \ .$$

The index j here can refer either to the coolant of smeared annulus j or to the fuel rods in annulus j .

The smearing necessary in this model cannot seriously impair the accuracy which is obtained. It intrudes only in the computation of G'_{ij} which is known to be quite insensitive to details of region i , and into the probability that a neutron born externally to r_i will collide again in a region external to r_i , after crossing the region internal to r_i . The latter probability will also be insensitive to the smearing model employed. The main source of error is in the Bonalumi approximation itself, which will certainly introduce errors into the probabilities for the outer moderator regions.

4.1 Reciprocity Relations

With the Bonalumi approach we need only calculate P_{jk} for $j \leqslant k$ since the remainder of the probabilities can be calculated from the relation:

$$V_j \Sigma_j P_{jk} = V_k \Sigma_k P_{kj} \ .$$

This relation ensures that P_{kj} will be calculated with the same accuracy as P_{jk}, a useful property for $j \leqslant i$, $k > i$ since we can tie P_{jk} fairly accurately through the correctly computed quantity P_{jr_i}.

In each of the methods discussed in Sections 2, 3, and 4 the outer boundary is assumed to be white reflecting. This allows the use of the surface/volume reciprocity relation:

$$\frac{1}{4}\ 2\pi R\ P_{Rj} = V_i\ \Sigma_i\ P_{iR}\ ,$$

to obtain a set of $P_{Rj} = \frac{2}{\pi R}\ V_i\ \Sigma_i\ P_{iR}$.

If we renormalise these so that Sum $P_{Rj} = 1$, the effect of reflection is a simple modification of the probabilities computed for a free outer boundary:

$$P_{ij} = P_{ij} + P_{iR}\ P_{Rj} \quad .$$

4.2 Treatment of Void Annuli in the Bonalumi Procedure

Annular voids are treated in the flux solution portion of our collision probability programme by omitting these regions from the calculation, as the collision rate and scattering source are both zero in the void. However, the void annuli must be treated explicitly in the calculation of the collision probabilities for the other annuli. The modifications necessary to achieve this are presented below. For full details of the original Bonalumi treatment the reader is referred to Bonalumi (1961) and Jonsson (1963).

The calculation may be divided into several stages, the first being the calculation of probabilities for the central cylinder. The self collision probability of the central region is the P_c function of Case, de Hoffman, and Placzek (1953):

$$P_{11} = P_c\ (\Sigma_1\ r_1)$$

$$P_{12} = (1 - P_{11})\ G_{12}$$

$$P_{13} = (1 - P_{11})\ (1 - G_{12})\ G_{13}$$

$$- - - - - - - - - - - - - - - -$$

$$P_{1j} = (1 - P_{11})(1 - G_{12})(1 - G_{13} - - - (1 - G_{1j-1})\ G_{1j} \quad ,$$

where the ring transmission probabilities $1 - G_{ij}$ are given by the relation

$$1 - G_{1j} = e^{-y_{ij}}$$

where

$$y_{1j} = \Sigma_j\ r_j\ \frac{\pi}{4}\ \tau \left[T\left(\frac{r_1}{r_j}\right) - \alpha_j\ T\left(\frac{r_1}{r_{j-1}}\right) \right] \quad ,$$

and

$$T(u) = \frac{2}{\pi}\left[\frac{\sin^{-1} u}{u} + \sqrt{1 - u^2} \right],$$

with

$$\alpha_j = \frac{r_{j-1}}{r_j}$$

and

$$\tau = \Sigma_2\ (r_2 - r_1) + \Sigma_3\ (r_3 - r_2) - - - + \frac{1}{2}\ \Sigma_j\ (r_j - r_{j-1}) \ .$$

The collision probabilities P_{j1} are obtained from the reciprocity relation:

$$P_{j1} = \frac{V_1 \Sigma_1 P_{1j}}{V_j \Sigma_j} .$$

Now if $\Sigma_1 = 0$ we obtain $P_{11} = 0$. The remaining ring probabilities G_{1j} and collision probabilities P_{1j} are correctly computed because Σ_1 does not appear explicitly in their evaluation. Straightforward application of the reciprocity relation yields $P_{j1} = 0$ as is expected.

If $\Sigma_1 \neq 0$ but $\Sigma_j = 0$ for some j, then $y_{1j} = 0$ and hence $G_{1j} = 0$. This gives correctly the result that $P_{1j} = 0$. However, we cannot use reciprocity to obtain P_{j1} since the computational result is indeterminate. However, if the quantity Σ_j is assumed small,

$$1 - G_{1j} = e^{-y_{1j}} .$$

$$\approx 1 - y_{1j} .$$

Hence

$$P_{1j} \approx (1 - P_{11})(1 - G_{12})(1 - G_{13}) - - - (1 - G_{1j-1})\, y_{1j} ,$$

and now applying reciprocity removes Σ_j from numerator and denominator:

$$P_{j1} = \frac{V_1 \Sigma_1}{V_j} (1-P_{11})(1-G_{12}) - - - (1-G_{1j-1})\; r_j \frac{\pi}{4} \tau \left[T\left(\frac{r_1}{r_j}\right) - \alpha_j\, T\left(\frac{r_1}{r_{j-1}}\right) \right] .$$

The calculation of the remaining collision probabilities is complicated by the need to consider the probabilities for neutrons crossing internal regions. Consider annulus i for which only P_{ij} $(j < i)$ are available, having been calculated by reciprocity from P_{ji}.

$$P_{ii} = P'_{ii} + \left\{ P^*_{i,i-1} - \underset{j<i}{\text{Sum}}\; P_{ij} \right\} G_{i-1,i} ,$$

where P'_{ii} = probability of collision in region i without crossing region internal to i,

$P^*_{i,i-1}$ = probability of crossing the boundary r_{i-1} ,

$$P^*_{i,i-1} = \frac{\pi r_{i-1}}{2 V_i \Sigma_i} G_{i-1,i} .$$

Here again if region i has $\Sigma_i = 0$ then $G_{i-1,i}$ must be expanded in powers of Σ_i to obtain a sensible result for $P^*_{i,i-1}$:

$$P'_{ii} = f_i - P^*_{i,i-1} G_{i-1,i} .$$

If $\Sigma_i = 0$, $P'_{ii} = 0$ is guaranteed by the form of f_i and the fact that $G_{i-1,i} = 0$.

The remainder of the collision probabilities can then be evaluated without difficulty.

5. A SYNTHETIC METHOD BASED ON THE BONALUMI APPROXIMATION

Use of the Bonalumi approximation in combination with numerical integration over regions containing rods gives reasonable agreement with the more exact results obtained purely from numerical integration and yields a substantial saving of computation time. In this section we explore the possibilities of a routine based solely on the Bonalumi approximation and considerations of neutron balance. Such a routine offers a reduction of two orders of magnitude in computation time and would make a cluster calculation possible in routine design calculations if the accuracy it achieved were adequate.

We assume that the rods on a given pitch circle can be surrounded by an annulus of coolant which completely encloses the rods, an assumption that is usually close to being satisfied in reality. The further assumption is made that the rods on a given pitch circle have the same symmetry properties, on the basis that the accuracy we will obtain is inconsistent with any attempt to distinguish rods with different symmetry properties on the same pitch circle.

The initial stage of the calculation is the same as that outlined in Section 4. The rods are volume-smeared into the appropriate annulus and a Bonalumi calculation is performed for the smeared annuli to obtain a set of collision probabilities which are labelled P'_{ij}. If both i and j refer to annuli which do not contain rods, the calculation of these probabilities is complete, apart from the calculation of reflection from the outer boundary of the cell, which is performed when the remaining rod probabilities have been resolved.

Next we consider the breakup of the probability P'_{ij} when annulus i is one which contains rods. All the rods in such an annulus are assumed indistinguishable and we define for the annulus a cell consisting of a rod (with whatever subdivisions of the rod that are specified) and an outer annulus of coolant equal in volume to the total volume of coolant in annulis i, divided by the number of rods in annulus i. Such a cell is annular and again we may apply the Bonalumi approximation to this system to obtain a set of collision probabilities P^2_{mn}.

P^2_{mn} = the probability computed by the Bonalumi approximation for regions m,n of the cell centred at the centre of the rod.

If the outer radius of this cell is taken to be R, the escape probability from region m is given by

$$P^2_{mR} = 1 - \underset{n}{\text{Sum}}\ P_{mn} \quad .$$

Further, using reciprocity, we can calculate the probability P^2_{Rm} that a neutron impinging isotropically on R will collide in annulus m:

$$P^2_{Rm} = \frac{2}{\pi R}\ V_m \Sigma_m\ P^2_{mR} \quad .$$

For neutrons which impinge on the cell and must collide in the cell we also need these probabilities normalised to unity:

$$P^3_{Rm} = P^2_{Rm} / \underset{m}{\text{Sum}}\ P^2_{Rm} \ .$$

Now consider the probability P'_{ij} and assume for the moment that region j is an annulus not containing rods.

If we assume that neutrons born in the annulus i are born in the cell which we have constructed to approximate annulus i then the probability P'_{ij} can be broken up as follows:

$$V_i P'_{ij} = \underset{m}{\text{Sum}}\ V_m P^2_{mR} P_{Rj},$$

where P_{Rj} is defined by the above equation to be the probability that a neutron emerging from annulus i, and hence, in our approximation, from the outer boundary R, will collide in annulus j. Re-arranging the above equation gives:

$$P_{Rj} = \frac{V_i P'_{ij}}{\underset{m}{\text{Sum}}\ V_m P^2_{mR}} \quad ,$$

and the individual probabilities P_{mj} are given immediately by the relation:

$$P_{mj} = P^2_{mR} P_{Rj} \ .$$

Treatment of the probabilities P_{jm} is equally direct. Here we assume that P_{jm} is given by the equation:

$$P_{mj} = P_{jR} \, P^3_{Rm} \quad ,$$

and the collision conservation relation:

$$P_{ji} = \underset{m}{\text{Sum}} \; P_{jm} = P_{jR} \; \underset{m}{\text{Sum}} \; P^3_{Rm} \quad ,$$

yields $P_{jR} = P_{ji}$ and hence the individual probabilities P_{jm}.

There remains only the computation of the self collision probabilities P_{mm}. The quantities P^2_{mR} are the probabilities of escape from region m so that the total escape probability for annulus i, based on our cell approximation, is:

$$1 - P^2_{ii} = \frac{\underset{m}{\text{Sum}} \; V_m \, P^2_{mR}}{\underset{m}{\text{Sum}} \; V_m} \quad .$$

We have from the initial Bonalumi computation on the smeared annulus i, a self collision probability P'_{ii} which must be conserved. The quantity Q defined by

$$Q = P'_{ii} - P^2_{ii} \quad ,$$

represents the net self collision probability lost in our assumption that annulus i can be replaced by an annular cell centred at the rod centre. This probability can be conserved by adjusting the collision probabilities in the following way:

$$P_{mn} = P^2_{mn} + P^2_{mR} \, P^3_{Rn} \, \frac{Q}{1 - P^2_{ii}} \quad .$$

Now recalculating the cell escape probability will demonstrate that probability is conserved.

$$\begin{aligned} P^3_{mR} &= 1 - \underset{n}{\text{Sum}} \; P_{mn} \\ &= 1 - \underset{n}{\text{Sum}} \; P^2_{mn} - P^2_{mR} \, \frac{Q}{1 - P^2_{ii}} \\ &= P^2_{mR} \left[1 - \frac{Q}{1 - P^2_{ii}} \right] . \end{aligned}$$

$$\begin{aligned} 1 - P_{ii} &= \frac{\underset{m}{\text{Sum}} \; V_m \, P^3_{mR}}{\underset{m}{\text{Sum}} \; V_m} \\ &= \frac{\underset{m}{\text{Sum}} \; V_m \, P^2_{mR}}{\underset{m}{\text{Sum}} \; V_m} \left[1 - \frac{Q}{1 - P^2_{ii}} \right] \\ &= \left[1 - P^2_{ii} \right] \left[1 - \frac{Q}{1 - P^2_{ii}} \right] \\ &= 1 - P^2_{ii} - Q \quad . \end{aligned}$$

$$P_{ii} = P^{2}_{ii} + Q$$

$$= P^{!}_{ii} \quad .$$

Thus we have established a relatively simple method of computing all the collision probabilities from the Bonalumi approximation, assuming that the outer boundary of the cluster cell is free. The usual application of reciprocity is employed to give isotropic reflection at the boundary for an array of similar cells.

5.1 Extension to Annuli which do not Completely Enclose the Rod

We expect our approximation will be good for loosely packed clusters where the smearing of the coolant in annulus i around the rods enclosed by i is physically reasonable. In tight clusters it may be impossible to define an annulus enclosing the rods on one pitch circle which does not intersect the rods on neighbouring pitch circles. We must rely on the user to define coolant annuli which most nearly satisfy this requirement and proceed with the calculation as though the requirement is satisfied. Thus a rod is assumed to be completely enclosed in an annulus if its centre is enclosed by the annulus. The effective cross section for such an annulus is computed by volume smearing all the rod into the annulus. This further approximation seems to be adequate on the problems tested where all the pitch circles come close to satisfying the separability requirement. We may expect poor results however for some power reactor clusters where neighbouring pitch circles are separated by distances considerably smaller than a rod diameter.

5.2 Accuracy Considerations

The synthetic approximation consists essentially of two approximations, firstly the smearing of rods to produce an effective cross section for an annulus containing rods and secondly the assumption that the coolant in a smeared annulus can be represented by an annulus surrounding the rod for what is essentially an unsmearing calculation. We cannot expect that the overall accuracy will be any better than a smeared transport calculation, though the division of events in a smeared annulus between events in the rod and events in the coolant may be better resolved than with a conventional unsmearing approach. It is also worth pointing out that reciprocity is no longer guaranteed in our approximation.

Suppose i is a smeared annulus with subdivisions indexed by m and that j is a simple unsmeared annulus. In the Bonalumi calculation with the smeared annuli, reciprocity is employed in the evaluation of P_{ji} for $j<i$:

$$V_i \Sigma_i P_{ij} = V_j \Sigma_j P_{ji} \quad .$$

We would like the reciprocity condition to remain valid for the individual subregions m of annulus i. That is, the equation:

$V_m \Sigma_m P_{mj} = V_j \Sigma_j P_{jm}$ should be true.

In our approximation:

$$P_{mj} = P^{2}_{mR} P_{Rj}$$

$$= P^{2}_{mR} \frac{\underset{m}{\text{Sum}}\ V_m}{\underset{m}{\text{Sum}}\ V_m P^{2}_{mR}} P_{ij} \quad .$$

Hence

$$P_{jm} = \frac{V_m \Sigma_m}{V_j \Sigma_j} P_{mR}^2 \frac{\underset{m}{\text{Sum}}\ V_m}{\underset{m}{\text{Sum}}\ V_m P_{mR}^2} P_{ij}$$

$$= \frac{V_m \Sigma_m P_{mR}^2}{\underset{m}{\text{Sum}}\ V_m P_{mR}^2} \frac{\underset{m}{\text{Sum}}\ V_m P_{ij}}{V_j \Sigma_j}$$

$$= \frac{V_m \Sigma_m P_{mR}^2}{\underset{m}{\text{Sum}}\ V_m P_{mR}^2} \frac{P_{ji}}{\Sigma_i}, \qquad (V_i = \underset{m}{\text{Sum}}\ V_m) .$$

What we are actually using is

$$P_{jm} = P_{ji} P_{Rm}^3 ,$$

where

$$P_{Rm}^3 = \frac{P_{Rm}}{\underset{m}{\text{Sum}}\ P_{Rm}^2}$$

$$= \frac{\frac{2}{\pi R} V_m \Sigma_m P_{mR}^2}{\underset{m}{\text{Sum}} \frac{2}{\pi R} V_m \Sigma_m P_{mR}^2} .$$

Hence

$$P_{jm} = \frac{V_m \Sigma_m P_{mR}^2}{\underset{m}{\text{Sum}}\ V_m \Sigma_m P_{mR}^2} P_{ji} .$$

These two expressions are equal only in the unlikely event that

$$\underset{m}{\text{Sum}}\ V_m \Sigma_m P_{mR}^2 = \Sigma_i \underset{m}{\text{Sum}}\ V_m P_{mR}^2 .$$

To conserve neutrons we have used the second of the two expressions for P_{jm}. It would be possible to resolve artificially the conflicting demands of reciprocity and summability, but in view of the other approximations in this method such a refinement is unwarranted.

6. NUMERICAL RESULTS AND CONCLUSIONS

Three clusters were selected for study, a 7 rod cluster, a 19 rod cluster and a 36 rod cluster. The 7 and 19 rod clusters are similar to some studied in the Canadian ZED 2 reactor, while the physical dimensions of the 36 rod cluster are those of a proposed natural steam generating heavy water (SGHW) design. The purpose of these calculations was to compare the different collision probability methods using the same regions and group structure. The rods were natural uranium, the cladding was assumed to be aluminium, and the coolant was assumed to be heavy water of the same composition as that of the bulk moderator. We used the same six group cross section set for each of the clusters, ignoring the obvious differences which would be present in realistic calculations for these systems.

No attempt is made here to compare with experiment; we are interested only in method comparison on clusters with representative physical dimensions and cross sections. Tables 1 – 3 specify the cluster dimensions used.

Results are presented in Tables 4 – 9 for three methods; full numerical integration, numerical integration with the Bonalumi approximation employed in the outer annuli, and the synthetic method based on the Bonalumi approximation. When the Bonalumi approximation is used with numerical integration, the numerical integration extends one annulus beyond the outermost annulus intersecting or enclosing a fuel rod. The possibility of altering this convention is available to the user, but in view of the results obtained there seems no reason to wish to do so. No results are presented for the Monte Carlo method, which proved less efficient than the full numerical integration. Since both of these methods purport to give an exact solution with the investment of sufficient computer time, the numerical integration routine will always be used in preference to the Monte Carlo routine which has served only as a check on the numerical integration.

The results of the numerical integration routine naturally depend on the number of lines and angles used in the integration. The user must specify the number of lines per annulus for the radial integration and these are selected to be equally spaced in radius across the width of the annulus. For the purposes of line mesh specification the presence of fuel rods in particular annuli is ignored. The selection of the number of lines per annulus is preferred for two reasons:

(1) Any increase in the number of lines automatically refines the probabilities for every annulus of the cluster. If the lines are equally spaced across the whole cluster this refinement cannot be ensured.

(2) An increase in the number of region subdivisions is automatically accompanied by an increase in the number of mesh lines in the region where the subdivision is made.

It is recognised that this philosophy may allow some probabilities to be calculated to better accuracy than their importance warrants. Against this, the inexperienced user is partially protected from obtaining anomalous results from a poor mesh choice.

Mesh lines are placed only on one half of the cluster, since in most clusters the rotational symmetry is such that tracks placed on the other half would yield identical region intercepts and collision probability contributions. For clusters with small numbers of rods on each pitch circle the number of angles in the angular integration should be increased, if necessary at the expense of the number of lines for annulus.

The programme will accept an angular integration interval of less than 2π, but in view of the restriction of the line mesh to one half of the cluster, use of intervals other than 2π should be avoided. The number of angles chosen should be relatively prime to the number of rods on each pitch circle so that duplication of tracks is avoided.

Tables 4, 6, and 8 show the variation in fluxes and eigenvalues resulting from different choices of line and angle mesh for the three clusters, and Table 8 also contains computation times for the 36 rod cluster. The computation time is proportional to the product of the number of lines per annulus and the number of angles in the integrations. The trends for all three clusters are much the same and the tables have been presented in full to enable the potential user to decide from his accuracy requirements what an acceptable mesh and angle specification might be.

Tables 5, 7, and 9 are repeat calculations where the outer annuli are calculated using the Bonalumi approximation while the annuli containing rods (and one more 'buffer' annulus) are calculated by numerical integration. The differences between these results and those of Tables 4, 6, and 8 are usually within acceptable limits, except for a trend in the outer moderator flux where the Bonalumi results for the group 6 flux are 3% high in the 36 rod cluster. Apart from this deficiency the approximation, which considerably reduces the computation time, must be recommended for realistic calculations. In the 36 rod cluster the time is roughly 0.4 of that required for full integration, the relative saving increasing with the number of moderator subdivisions.

Finally, at the end of each of Tables 4 – 9 we have presented the results obtained from the synthetic calculation. The speed of this calculation is, by cluster standards, quite outstanding. Whether the results are any better than one can obtain from a ring smeared WDSN calculation of the

type available in the WIMS code (Askew et al. 1966) we are not in a position to determine at present. When the collision probability portion of the calculation takes negligible time, we have previously shown (Doherty 1969 b) that the breakdown point between WDSN and the collision probability flux convergence occurs at about 4 energy groups. For more than 4 energy groups the collision probability method is superior on computational speed because of the more sophisticated acceleration techniques which are employed.

It must be remembered, however, that errors in the Bonalumi approximation do not allow mesh regions to be refined indefinitely to remove the dependence of the collision probability method on the flat flux assumption. Beyond a certain number of subdivisions, the changes in the estimates of fluxes and eigenvalue are caused mainly by the errors in the approximation, rather than by improvements in the spatial flux representation. This restriction applies to the synthetic method and to the numerical integration, Bonalumi combination.

The synthetic method based on the Bonalumi approximation bears some resemblance to the method described by Leslie and Jonsson (1965). The results obtained from the two methods seem to have roughly similar accuracy and the computation times are similar. The method presented here, while less plausible on physical grounds, allows the specific inclusion of canning material and subdivision of the fuel pins in a straightforward fashion. By contrast, pin subdivisions can be included in the Leslie and Jonsson method only with difficulty.

7. REFERENCES

Askew, J.R., Fayers, F.J., Kemshell, P.B. (1966). – A general description of the lattice code WIMS. J. Brit. Nucl. Energy Soc. 5 (4): 564.

Beardwood, J.E., Clayton, A.J. and Pull, I.C. (1965). – The solution of the transport equation by collision probability methods. ANL–7050 p.93.

Bonalumi, R. (1961). – Neutron first collision probabilities in reactor physics. Energia Nucleare 8, 5, 326.

Case, K.M., de Hoffman, F. and Placzek, G. (1953). – Introduction to the Theory of Neutron Diffusion. Vol. 1, LASL report, U.S. Govt. Printing Office.

Clayton, A.J. (1964). – Some rational approximations for the K_{i3} and K_{i4} functions. J. Nucl. Energy 18: 84.

Doherty, G. (1969 a). – Solution of the multigroup collision probability equations. AAEC/E197.

Doherty, G. (1969 b). – Solution of some problems by collision probability methods. AAEC/E199.

Gargantini, I. and Pomentale, T. (1964). – Rational Chebyshev approximations to the Bessel function integrals $K_{is}(x)$. Comm. A.C.M. 7 (12): 727.

Jonsson, A. (1963). – Theseus – A one group collision probability routine for annular systems. AEEW R253.

Leslie, D.C. and Jonsson, A. (1965). – The calculation of collision probabilities in cluster-type fuel elements. Nucl. Sci. Eng. 23 (3): 272.

McCulloch, D.B., Doherty, G. and Hesse, E. (1968). – Monte Carlo calculations (one-group) of U238/U235 fission ratios in rod-cluster fuel elements. AAEC/TM432.

Pull, I.C. (1962). – Paper entitled 'Special techniques in Monte Carlo' in Numerical Solutions of Ordinary and Partial Differential Equations, L. Fox editor. Pergamon Press.

Pull, I.C. (1963). – The solution of equations arising from the use of collision probabilities. AEEW–M355.

Woodcock, E.R., Murphy, T., Hemmings, P.J. and Langworth, T.C. (1965). – Techniques used in the GEM code for Monte Carlo neutronics calculations in reactors and other systems of complex geometry. ANL–7050 p.557.

TABLE 1

7 ROD CLUSTER SPECIFICATION

Central rod

+ 6 rods on pitch circle of radius 2.6666 cm

	Outer Radius (cm)	Material
Rod subdivisions	1.200	nat U metal
	1.219	void
	1.2698	Al
Coolant subdivisions	1.3333	D_2O
	3.9364	D_2O
	4.1275	D_2O
Pressure tube	5.0175	Al
Insulating gap	5.08	void
Calandria tube	6.50	Al
Moderator subdivisions	7.50	D_2O
	8.50	D_2O
	9.50	D_2O
	10.50	D_2O
	11.50	D_2O

TABLE 2

19 ROD CLUSTER SPECIFICATION

Central rod

+ 6 rods on pitch circle of radius 1.6488 cm

+ 12 rods on pitch circle of radius 3.2976 cm

	Outer Radius (cm)	Material
Rod subdivisions	0.7105	nat U metal
	0.7155	void
	0.7609	Al
Coolant subdivisions	0.82434	D_2O
	2.4732	D_2O
	4.1275	D_2O
Pressure tube	5.0175	Al
Insulating gap	5.08	void
Calandria tube	6.50	Al
Moderator subdivisions	7.50	D_2O
	8.50	D_2O
	9.50	D_2O
	10.50	D_2O
	11.50	D_2O

TABLE 3

36 ROD CLUSTER SPECIFICATION

6 rods on pitch circle of radius 1.8895 cm

12 rods on pitch circle of radius 3.6475 cm

18 rods on pitch circle of radius 5.5005 cm

	Outer Radius (cm)	Material
Rod subdivisions	0.846	nat U metal
	0.8935	Al
Coolant subdivisions	0.379	Al
	0.73	D_2O
	0.862	Al
	2.6763	D_2O
	4.511	D_2O
	6.3998	D_2O
Pressure tube	6.809	Al
Insulating gap	8.4735	void
Calandria tube	8.5535	Al
Moderator subdivisions	10.3	D_2O
	12.0	D_2O
	13.8	D_2O
	15.6	D_2O
	17.4	D_2O
	19.16414	D_2O

TABLE 4

7 ROD CLUSTER RESULTS FOR FULL NUMERICAL INTEGRATION

Number of lines/ annulus	Number of angles	k	Group 1 fuel 1 flux	Group 6 fuel 1 flux	Group 1 fuel 2 flux	Group 6 fuel 2 flux	Group 1 outer moderator flux	Group 6 outer moderator flux
1	1	0.95741	0.09295	0.04430	0.06996	0.06097	0.01345	0.15028
1	5	0.95349	0.08511	0.04321	0.07498	0.05971	0.01347	0.14027
1	7	0.95722	0.08838	0.04669	0.07192	0.06027	0.01345	0.14788
1	11	0.95445	0.08651	0.04360	0.07393	0.05997	0.01347	0.14233
2	1	0.96103	0.07683	0.04920	0.07593	0.06019	0.01345	0.15223
2	5	0.96167	0.08293	0.04727	0.07211	0.06111	0.01349	0.15453
2	7	0.96102	0.08288	0.04721	0.07269	0.06096	0.01351	0.15432
2	11	0.96160	0.08157	0.04770	0.07287	0.06093	0.01348	0.15419
4	1	0.96262	0.07829	0.04770	0.07168	0.06154	0.01351	0.15935
4	5	0.96311	0.08174	0.04616	0.07141	0.06183	0.01346	0.15950
4	7	0.96242	0.07958	0.04595	0.07234	0.06163	0.01350	0.15773
4	11	0.96307	0.08094	0.04638	0.07143	0.06180	0.01347	0.15939
8	1	0.96271	0.07771	0.04556	0.07217	0.06182	0.01351	0.15848
8	5	0.96297	0.08110	0.04494	0.07206	0.06193	0.01348	0.15915
8	7	0.96268	0.07963	0.04511	0.07222	0.06186	0.01348	0.15885
8	11	0.96265	0.08010	0.04503	0.07209	0.06189	0.01349	0.15871
16	1	0.96261	0.07769	0.04613	0.07221	0.06176	0.01348	0.15976
16	5	0.96265	0.08122	0.04494	0.07202	0.06194	0.01347	0.16004
16	7	0.96282	0.07967	0.04536	0.07207	0.06189	0.01347	0.15964
16	11	0.96259	0.08043	0.04528	0.07199	0.06190	0.01347	0.16006
Synthetic		0.96362	0.07896	0.04563	0.07069	0.06200	0.01353	0.16001

TABLE 5

7 ROD CLUSTER RESULTS FOR BONALUMI AND NUMERICAL INTEGRATION MIXTURE

Number of lines/ annulus	Number of angles	k	Group 1 fuel 1 flux	Group 6 fuel 1 flux	Group 1 fuel 2 flux	Group 6 fuel 2 flux	Group 1 outer moderator flux	Group 6 outer moderator flux
1	1	0.96026	0.09185	0.04352	0.06985	0.06181	0.01349	0.15977
1	5	0.95909	0.08487	0.04524	0.07428	0.06071	0.01352	0.15347
1	7	0.96053	0.08744	0.04654	0.07168	0.06114	0.01350	0.15864
1	11	0.95943	0.08603	0.04489	0.07337	0.06095	0.01352	0.15478
2	1	0.96352	0.07693	0.05040	0.07576	0.06055	0.01347	0.15936
2	5	0.96350	0.08263	0.04723	0.07216	0.06145	0.01351	0.15915
2	7	0.96330	0.08263	0.04737	0.07272	0.06132	0.01353	0.15894
2	11	0.96349	0.08132	0.04783	0.07289	0.06128	0.01350	0.15940
4	1	0.96374	0.07828	0.04759	0.07191	0.06164	0.01352	0.16133
4	5	0.96393	0.08174	0.04601	0.07165	0.06192	0.01347	0.16191
4	7	0.96377	0.07972	0.04627	0.07249	0.06173	0.01350	0.16036
4	11	0.96387	0.08093	0.04624	0.07166	0.06188	0.01348	0.16190
8	1	0.96384	0.07793	0.04589	0.07235	0.06185	0.01351	0.16026
8	5	0.96399	0.08128	0.04516	0.07227	0.06197	0.01348	0.16117
8	7	0.96372	0.07983	0.04541	0.07241	0.06190	0.01348	0.16111
8	11	0.96387	0.08030	0.04532	0.07228	0.06194	0.01349	0.16088
16	1	0.96351	0.07787	0.04631	0.07244	0.06178	0.01348	0.16155
16	5	0.96359	0.08140	0.04510	0.07226	0.06196	0.01346	0.16177
16	7	0.96369	0.07986	0.04556	0.07230	0.06191	0.01347	0.16156
16	11	0.96354	0.08060	0.04543	0.07223	0.06191	0.01347	0.16168
Synthetic		0.96362	0.07896	0.04563	0.07069	0.06200	0.01353	0.16001

TABLE 6

19 ROD CLUSTER RESULTS FOR FULL NUMERICAL INTEGRATION

Number of lines / annulus	Number of angles	k	Group 1 fuel 1 flux	Group 6 fuel 1 flux	Group 1 fuel 2 flux	Group 6 fuel 2 flux	Group 1 fuel 3 flux	Group 6 fuel 3 flux	Group 1 outer moderator flux	Group 6 outer moderator flux
1	1	0.95961	0.08152	0.04692	0.06859	0.04861	0.06813	0.07120	0.01391	0.14336
1	5	0.95825	0.07892	0.04835	0.08016	0.05281	0.06587	0.06825	0.01386	0.14311
1	7	0.96047	0.08413	0.04997	0.06969	0.05183	0.06589	0.06963	0.01388	0.14630
1	11	0.95896	0.08006	0.04885	0.07819	0.05280	0.06527	0.06865	0.01384	0.14461
2	1	0.96404	0.07803	0.04978	0.07771	0.05752	0.06112	0.06851	0.01384	0.15623
2	5	0.96548	0.08140	0.05045	0.07296	0.05502	0.06217	0.07025	0.01386	0.15842
2	7	0.96367	0.07727	0.04713	0.07451	0.05200	0.06492	0.07086	0.01384	0.15193
2	11	0.96512	0.08016	0.05000	0.07379	0.05542	0.06203	0.06994	0.01384	0.15752
4	1	0.96477	0.06903	0.04348	0.07282	0.05201	0.06385	0.07193	0.01385	0.15501
4	5	0.96521	0.07118	0.04306	0.07263	0.05097	0.06461	0.07249	0.01386	0.15557
4	7	0.96473	0.07109	0.04299	0.07323	0.05188	0.06499	0.07189	0.01385	0.15590
4	11	0.96508	0.07022	0.04349	0.07250	0.05110	0.06467	0.07237	0.01386	0.15535
8	1	0.96452	0.07388	0.04675	0.07112	0.05148	0.06439	0.07199	0.01385	0.15678
8	5	0.96481	0.07595	0.04596	0.07264	0.05174	0.06448	0.07184	0.01384	0.15698
8	7	0.96499	0.07535	0.04621	0.07240	0.05189	0.06460	0.07179	0.01384	0.15701
8	11	0.96475	0.07528	0.04623	0.07226	0.05166	0.06443	0.07189	0.01385	0.15698
16	1	0.96454	0.07347	0.04630	0.07203	0.05213	0.06386	0.07171	0.01385	0.15655
16	5	0.96482	0.07554	0.04554	0.07292	0.05183	0.06428	0.07183	0.01384	0.15678
16	7	0.96495	0.07490	0.04579	0.07254	0.05192	0.06456	0.07178	0.01384	0.15675
16	11	0.96472	0.07478	0.04580	0.07276	0.05192	0.06423	0.07177	0.01384	0.15672
Synthetic		0.96578	0.07283	0.04647	0.07261	0.05186	0.06542	0.07167	0.01379	0.15822

TABLE 7

19 ROD CLUSTER RESULTS FOR BONALUMI AND NUMERICAL INTEGRATION MIXTURE

Number of lines / annulus	Number of angles	k	Group 1 fuel 1 flux	Group 6 fuel 1 flux	Group 1 fuel 2 flux	Group 6 fuel 2 flux	Group 1 fuel 3 flux	Group 6 fuel 3 flux	Group 1 outer moderator flux	Group 6 outer moderator flux
1	1	0.96297	0.08173	0.04752	0.06904	0.05088	0.06757	0.07117	0.01397	0.15277
1	5	0.96244	0.07829	0.04906	0.07955	0.05319	0.06570	0.06925	0.01393	0.15189
1	7	0.96361	0.08343	0.04948	0.07307	0.05260	0.06573	0.07025	0.01395	0.15390
1	11	0.96258	0.07932	0.04902	0.07767	0.05312	0.06516	0.06958	0.01394	0.15262
2	1	0.96542	0.07719	0.04880	0.07656	0.05541	0.06172	0.06983	0.01390	0.15768
2	5	0.96634	0.08058	0.04893	0.07251	0.05391	0.06260	0.07095	0.01392	0.15932
2	7	0.96533	0.07706	0.04711	0.07440	0.05214	0.06495	0.07124	0.01388	0.15619
2	11	0.96605	0.07934	0.04866	0.07322	0.05417	0.06247	0.07075	0.01390	0.15903
4	1	0.96554	0.06946	0.04436	0.07287	0.05202	0.06392	0.07201	0.01388	0.15768
4	5	0.96603	0.07169	0.04393	0.07284	0.05126	0.06464	0.07242	0.01389	0.15802
4	7	0.96563	0.07155	0.04389	0.07334	0.05202	0.06506	0.07188	0.01387	0.15801
4	11	0.96593	0.07074	0.04441	0.07271	0.05141	0.06469	0.07229	0.01389	0.15776
8	1	0.96518	0.07401	0.04673	0.07136	0.05182	0.06446	0.07188	0.01395	0.15845
8	5	0.96481	0.07595	0.04596	0.07264	0.05174	0.06448	0.07184	0.01384	0.15698
8	7	0.96522	0.07538	0.04612	0.07251	0.05196	0.06472	0.07183	0.01387	0.15856
8	11	0.96547	0.07536	0.04619	0.07242	0.05184	0.06454	0.07187	0.01387	0.15851
16	1	0.96525	0.07354	0.04631	0.07213	0.05217	0.06398	0.07175	0.01388	0.15794
16	5	0.96482	0.07554	0.04554	0.07292	0.05182	0.06428	0.07183	0.01384	0.15678
16	7	0.96566	0.07498	0.04583	0.07263	0.05199	0.06467	0.07182	0.01387	0.15835
16	11	0.96544	0.07485	0.04584	0.07283	0.05196	0.06435	0.07183	0.01387	0.15830
Synthetic		0.96578	0.07283	0.04647	0.07261	0.05186	0.06542	0.07167	0.01379	0.15822

TABLE 8

36 ROD CLUSTER RESULTS FOR FULL NUMERICAL INTEGRATION ROUTINE

Number of lines / annulus	Number of angles	k	Group 1 fuel 1 flux	Group 6 fuel 1 flux	Group 1 fuel 2 flux	Group 6 fuel 2 flux	Group 1 fuel 3 flux	Group 6 fuel 3 flux	Group 1 outer moderator flux	Group 6 outer moderator flux	Time for probability calc. minutes
1	1	1.0946	0.03070	0.02069	0.02848	0.02226	0.02914	0.03496	0.00255	0.12887	4
1	5	1.0753	0.03563	0.01490	0.03507	0.02029	0.03207	0.03507	0.00251	0.11487	15
1	7	1.0755	0.03513	0.01485	0.03470	0.02008	0.03225	0.03527	0.00250	0.11501	21
1	11	1.0753	0.03510	0.01481	0.03456	0.02011	0.03216	0.03527	0.00250	0.11494	32
2	1	1.0774	0.03542	0.01309	0.03647	0.02030	0.03157	0.03582	0.00250	0.11517	6
2	5	1.0805	0.03369	0.01477	0.03349	0.02059	0.03130	0.03575	0.00251	0.11805	30
2	7	1.0810	0.03315	0.01487	0.03353	0.02053	0.03115	0.03584	0.00250	0.11842	40
2	11	1.0810	0.03325	0.01480	0.03364	0.02059	0.03112	0.03581	0.00251	0.11840	64
4	1	1.0840	0.03436	0.01445	0.03478	0.02132	0.03073	0.03563	0.00250	0.11968	13
4	5	1.0827	0.03250	0.01478	0.03349	0.02080	0.03094	0.03593	0.00250	0.11964	59
4	7	1.0826	0.03265	0.01481	0.03344	0.02076	0.03085	0.03595	0.00251	0.11973	82
4	11	1.0823	0.03269	0.01473	0.03335	0.02068	0.03099	0.03599	0.00250	0.11947	128
8	1	1.0852	0.03363	0.01479	0.03385	0.02061	0.03111	0.03617	0.00249	0.12070	26
8	5	1.0834	0.03252	0.01483	0.03331	0.02079	0.03082	0.03603	0.00251	0.12028	117
8	7	1.0831	0.03265	0.01484	0.03315	0.02077	0.03086	0.03603	0.00251	0.12019	163
8	11	1.0830	0.03250	0.01476	0.03332	0.02077	0.03084	0.03604	0.00251	0.12015	256
16	1	1.0848	0.03353	0.01467	0.03393	0.02055	0.03130	0.03618	0.00250	0.12025	52
16	5	1.0831	0.03257	0.01476	0.03330	0.02066	0.03093	0.03610	0.00250	0.12017	234
16	7	1.0830	0.03254	0.01476	0.03331	0.02072	0.03089	0.03606	0.00250	0.12016	326
16	11	1.0831	0.03254	0.01478	0.03326	0.02071	0.03090	0.03607	0.00250	0.12019	512
Synthetic		1.0799	0.03200	0.01400	0.03438	0.02024	0.03189	0.03617	0.00243	0.12312	0.06

TABLE 9

36 ROD CLUSTER RESULTS FOR BONALUMI AND NUMERICAL INTEGRATION MIXTURE

Number of lines / annulus	Number of angles	k	Group 1 fuel 1 flux	Group 6 fuel 1 flux	Group 1 fuel 2 flux	Group 6 fuel 2 flux	Group 1 fuel 3 flux	Group 6 fuel 3 flux	Group 1 outer moderator flux	Group 6 outer moderator flux	Time for probability calc. minutes
1	1	1.0761	0.03239	0.01355	0.03557	0.02042	0.03253	0.03563	0.00250	0.11969	1
1	5	1.0770	0.03527	0.01494	0.03582	0.02100	0.03167	0.03480	0.00249	0.12058	6
1	7	1.0777	0.03470	0.01508	0.03512	0.02089	0.03150	0.03500	0.00251	0.12060	8
1	11	1.0766	0.03449	0.01449	0.03594	0.02072	0.03226	0.03506	0.00249	0.12001	12
2	1	1.0793	0.03555	0.01346	0.03644	0.02049	0.03150	0.03581	0.00249	0.12001	3
2	5	1.0806	0.03371	0.01482	0.03353	0.02074	0.03128	0.03567	0.00249	0.12198	13
2	7	1.0809	0.03316	0.01491	0.03356	0.02062	0.03116	0.03579	0.00249	0.12231	17
1	11	1.0808	0.03327	0.01485	0.03367	0.02067	0.03112	0.03576	0.00250	0.12216	26
4	1	1.0834	0.03430	0.01440	0.03470	0.02109	0.03083	0.03574	0.00249	0.12280	5
4	5	1.0820	0.03250	0.01476	0.03349	0.02076	0.03099	0.03590	0.00249	0.12283	24
4	7	1.0818	0.03267	0.01482	0.03345	0.02073	0.03090	0.03589	0.00249	0.12281	33
4	11	1.0817	0.03272	0.01475	0.03338	0.02069	0.03102	0.03593	0.00249	0.12281	52
8	1	1.0842	0.03361	0.01470	0.03386	0.02053	0.03119	0.03616	0.00248	0.12362	10
8	5	1.0823	0.03256	0.01482	0.03334	0.02075	0.03088	0.03595	0.00249	0.12310	47
8	7	1.0821	0.03267	0.01481	0.03320	0.02075	0.03091	0.03593	0.00249	0.12296	66
8	11	1.0821	0.03253	0.01476	0.03335	0.02073	0.03099	0.03597	0.00249	0.12305	104
16	1	1.0840	0.03359	0.01471	0.03398	0.02056	0.03134	0.03608	0.00248	0.12326	20
16	5	1.0823	0.03261	0.01477	0.03334	0.02066	0.03098	0.03601	0.00249	0.12315	93
16	7	1.0822	0.03257	0.01476	0.03334	0.02069	0.03096	0.03599	0.00249	0.12315	131
16	11	1.0821	0.03258	0.01478	0.03330	0.02070	0.03095	0.03597	0.00249	0.12307	207
Synthetic		1.0799	0.03200	0.01400	0.03438	0.02024	0.03189	0.03617	0.00243	0.12312	0.06

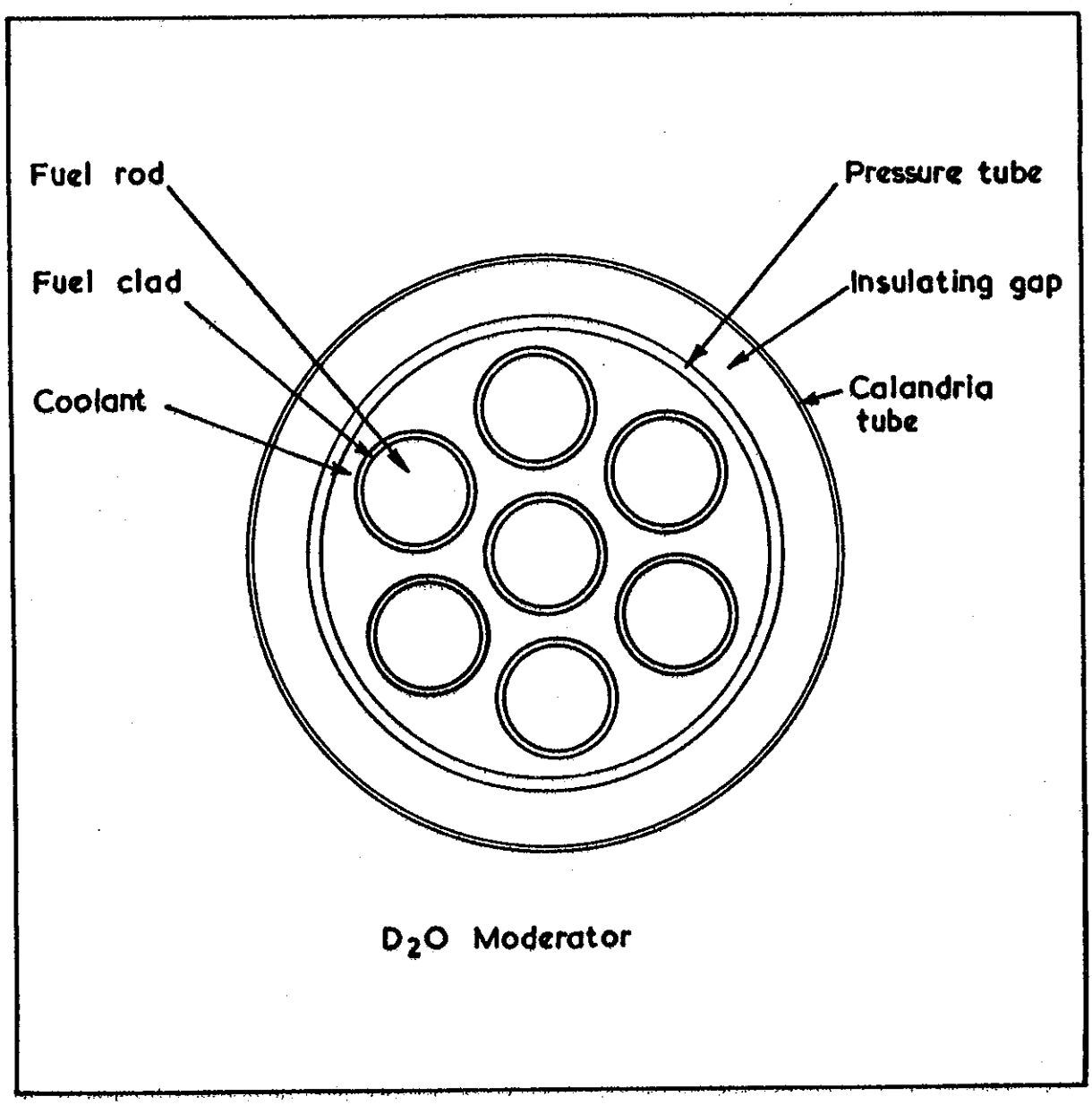

FIGURE 1. A TYPICAL CLUSTER LATTICE CELL